Calculations of the time structure of incidence of extensive air showers

1975 J. Phys. A: Math. Gen. 8 838

(http://iopscience.iop.org/0305-4470/8/5/019)

J. Phys. A: Math. Gen., Vol. 8, No. 5, 1975. Printed in Great Britain.

Calculations of the time structure of incidence of extensive air showers

J Lapikens

Department of Physics, University of Leeds, Leeds LS2 9JT, UK

Received 10 October 1974, in final form 15 November 1974

Abstract. A series of model calculations is described and the results for average proton-initiated extensive air showers of about 10^{18} eV are compared with those of other model calculations and with a wide range of experimental data, including the work of Watson and Wilson on the time structure of the shower front of EAS. Particular care has been taken to allow the model calculations to be matched with the experimental data and the conclusion of those authors that protons are present in the primary cosmic ray beam at about 10^{18} eV is supported. Further work is suggested to test whether the fluctuations found experimentally can be explained on other hypotheses.

1. Introduction

It has long been recognized that a detailed study of the time structure of incidence of extensive air showers (EAS) upon detectors may provide a possible method of yielding information on the longitudinal development of EAS (Linsley and Scarsi 1962, Wilson *et al* 1963). Recent work at Haverah Park using this technique (Lapikens *et al* 1973, Watson and Wilson 1974) has demonstrated, without recourse to detailed model calculations, that far from the axis fluctuations exist between showers which are significantly greater than expected on the basis of measurement errors and statistical sampling effects alone.

Interpretation of the fluctuations observed in these showers (primary energy about 10^{18} eV) was difficult because no shower model calculations which accurately treated the response of the deep water-Čerenkov detectors to the shower complex were available. In this paper the results of model calculations which pay particular attention to this problem are described and it is shown for two shower models, which appear to explain many aspects of showers of energy above 10^{17} eV, that the data of Watson and Wilson (1974) are consistent with a primary beam which is predominantly protonic. Further model calculations require to be undertaken before this conclusion can be regarded as fully established and some future lines of approach to the problem are outlined.

2. Description of the calculations

The properties of the EAS initiated by cosmic rays of energy above 10^{17} eV can only be calculated by using a highly simplified representation of the shower generation processes. Studies at Leeds extended over a period of several years (Hillas *et al* 1971) have led to a representation which is capable of predicting accurately the values of air shower

observables and which, by suitable choice of high energy interaction parameters, gives agreement with experimental data. The distinct stages involved in the calculations of the deep water-Čerenkov detector time profile are illustrated in figure 1.

The growth of the pion cascade is calculated by moving in successive small steps through the atmosphere using a technique described in detail by Marsden (1971). This stage of the calculation is one-dimensional and is adequate for the calculation of observables at large axial distances (greater than 100 m) since the pion cascade remains within about 10 m of the shower axis. The output of this stage of the calculation

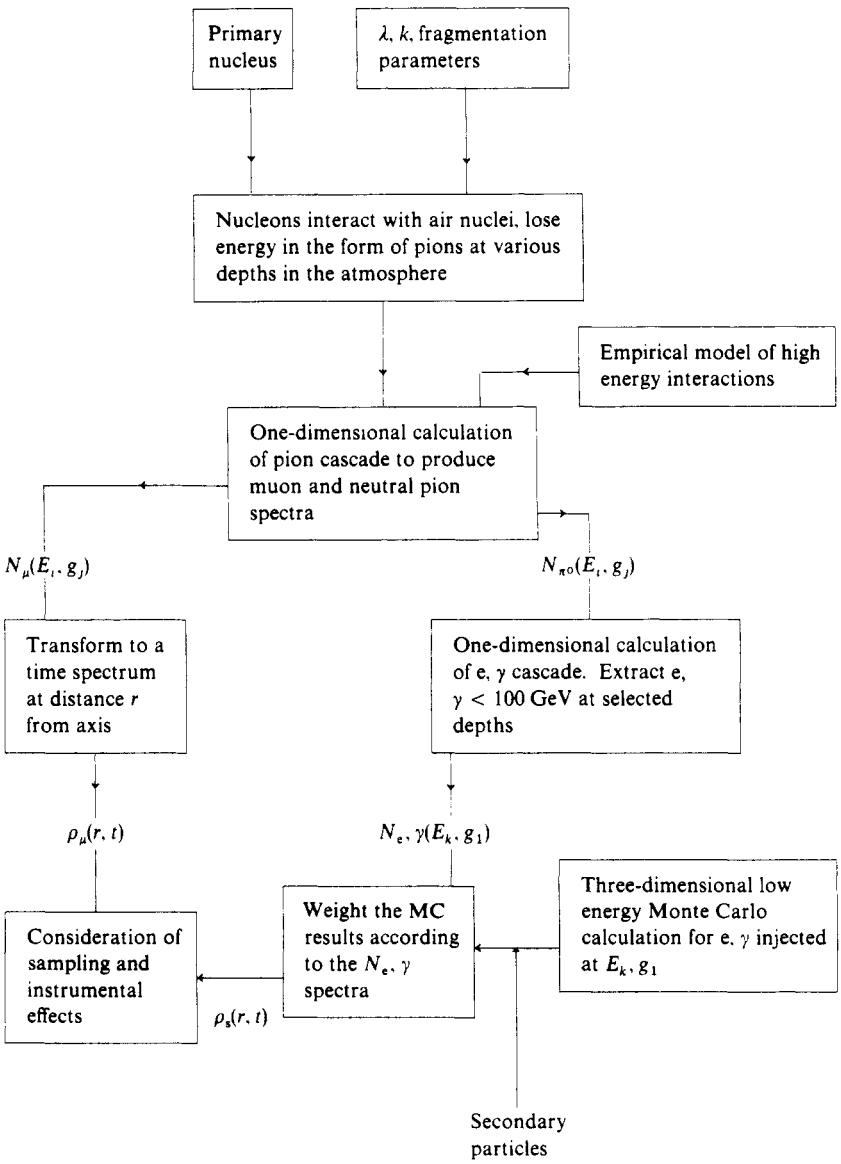

Figure 1. Block diagram illustrating the steps in model calculations of deep water-Čerenkov detector time profiles.

is in the form of muon and neutral pion energy production–height spectra—$N_\mu(E_i, g_j)$, $N_\pi^0(E_i, g_j)$ where E_i is the energy of the particle at depth g_j.

Muons are highly penetrating and not strongly scattered by the atmosphere; their contribution to the detector signal can therefore be straightforwardly obtained as follows.

The density contribution at the distance r from the axis for a single muon produced at a depth g_j with energy E_i can be given in the form:

$$p_{ij} = (2\pi r)^{-1} F(E_i, g_j, r) S(E_i, g_j, r) C(E_i, g_j, r).$$

F is derived from the transverse momentum distribution of the pions which decayed into muons and is the dominant cause of lateral spread.

S is the fraction of muons which do not decay in flight; typically muon decay reduces the muon density by 25%. The muon decay product is an electron which initiates an electromagnetic cascade which can produce an appreciable signal in the detector. In the present calculation this contribution to the detector signal has been ignored. If more accurate calculations, ie particle densities accurate to better than 7%, are required this contribution should be included in future.

C is the flattening effect of Coulomb scattering; the effect on densities is small (less than 2%) and can be neglected (Hillas 1965).

The time delay of the muon is

$$q_{ij} = t_g(g_j, r) + t_v(E_i, g_j, r) + t_c(E_i, g_j, r) + t_m(E_i, g_j, r),$$

where the geometrical delay t_g is the dominant cause of muon delays at large distances from the shower axis.

The delay t_v which arises from muons travelling at less than the speed of light also makes a noticeable contribution (typically 30% to the mean delay at $r = 400$ m).

The delays t_c, t_m due to Coulomb scattering and geomagnetic effects respectively have been calculated only to an accuracy of about 25%, but their contribution to the total delays is so small (about 5% at $r = 400$ m) that a more accurate calculation is unnecessary at this stage of the work.

The time distribution of the muon density resulting from a given muon production spectrum $N(E_i, g_j)$ is obtained by summation:

$$\rho(r, t) = \sum_{ij} N_{ij} p_{ij} \delta(t - q_{ij})$$

and table 1 gives a sample of values of the variables in the above equations calculated using one particular shower model (see below). Formulae for calculating F, S, t_v etc

Table 1. Muon time parameters and densities at 400 m from the axis for a source height of $g = 633\ \mathrm{g\,cm^{-2}}$ (3·81 km). E, E_{s1} (GeV) represent the muon energy at 3·81 km and at the ground; S is the survival probability; t_g, t_v, t_c, t_m and q_{ij} (ns) are defined in the text; d_{ij} is the relative density contribution arising from muons produced in the range $g \rightarrow g - 10\ \mathrm{g\,cm^{-2}}$. $(E/1{\cdot}15) \rightarrow (E \times 10^{1/8}/1{\cdot}15)$ GeV.

E	E_{s1}	S	t_g	t_v	t_c	t_m	q_{ij}	d_{ij}
1·15	0·35	0·41	70	512	23	1	607	6·6
2·05	1·24	0·69	70	22	3	0	94	20·1
3·64	2·83	0·83	70	2	1	0	73	21·2
6·47	5·67	0·91	70	0	0	0	70	7·3
11·5	10·7	0·95	70	0	0	0	70	0·5

are given in Lapikens (1974); these were derived for a muon propagating in an isothermal atmosphere and assuming a constant ionization loss of 2 MeV g^{-1} cm^{-2}.

The neutral pions lead to electromagnetic particle cascades. These propagate through the atmosphere in a rather complex manner, being affected at lower energies (less than 1 GeV) by multiple Coulomb scattering and a variety of electromagnetic processes (bremsstrahlung, pair production, Compton effect and ionization loss). It would appear that the problem of determining the dispersion in time and space of the cascade particles can be realistically approached only by the use of Monte Carlo techniques. It is possible to simulate directly all the processes involved in the propagation of an electromagnetic cascade through the atmosphere, and the accuracy attained is limited by the correctness with which the relevant cross sections are represented in the computer program and by the statistical weight of the results. The disadvantage of the method is that to obtain statistically significant results a large number of simulations, which require a large amount of computer time, is required.

A computer program written by Baxter (1969) and further developed by Marsden (1971) was designed specifically to predict the characteristics of the large EAS observed by the Haverah Park, Volcano Ranch and Chacaltaya arrays as to the electromagnetic component at large axial distances. Particular care was taken to ensure that no errors occurred in the implementation of the calculations and it is believed that the results are essentially correct.

The program has been used to simulate the secondary particles which reach ground level when electrons and photons of energies 1, 3·16, 10, 31·6, 100 GeV are injected at atmospheric depths of 80, 160, 240, ... g cm^{-2}. Such secondary subshowers are stored on magnetic tape or disc and are subsequently used to build up particle distributions for full air showers.

In order to make use of these Monte Carlo results, the neutral pion number spectrum must be represented in terms of an equivalent spectrum of electrons and photons whose energies and depths correspond to the starting points for the full Monte Carlo calculations. This is achieved by a one-dimensional calculation of the cascade growth. Only bremsstrahlung and pair production processes are considered since these dominate at energies above 1 GeV. The cascade growth is determined numerically from the pair production and bremsstrahlung cross sections by stepping in 1 g cm^{-2} intervals through the atmosphere. Whenever a depth at which full Monte Carlo calculations are available is reached, particles of energy below 100 GeV are removed from the cascade. Thus the energy of the cascade is extracted in a form suitable for its continuation by the use of the previously calculated Monte Carlo results, and the numbers of these extracted particles are then used as weighting functions to convert the stored secondary particle distributions into particle distributions in air showers which would be recorded in 120 cm deep water-Čerenkov detectors.

3. Calculations for an average proton shower

The previously outlined techniques have been used to determine the average characteristics of showers initiated by protons of mean free path 80 g cm^{-2} and inelasticity 0·44. The secondary particle spectrum (of pions) produced by such primary interactions was determined by stepping through the atmosphere in 2 g cm^{-2} increments, and the pion cascade growth was calculated using model A (Hillas *et al* 1971). This model was used so that the computations could be checked against the detailed report of results given by

Marsden (1971) which deals exclusively with model A. Details of model A (and model E, see later) are given in table 2.

A sample of results for a $1{\cdot}15 \times 10^{18}$ eV vertical shower is shown in figure 2 and table 3. The normalized muon component time delays are plotted in figure 2(*a*), the soft component time delays in figure 2(*b*) and the lateral distributions are compared in table 3.

Table 2. Parameters in models A and E.

	Model A	Model E
Proton interaction length	80 g cm^{-2}	80 g cm^{-2}
Inelasticity for average showers	0·44	0·44
Pion interaction length	100 g cm^{-2}	100 g cm^{-2}
Multiplicity	$3{\cdot}43E_r^{1/4}$ to $3{\cdot}78E_r^{1/4}$	$2{\cdot}56E_r^{1/4}$
Secondary pion energy spectrum	$\frac{1}{T}\exp\left(\frac{E}{T}\right)+\frac{2}{U}\exp\left(\frac{E}{U}\right)$	$\frac{1}{T}\exp\left(\frac{E}{T}\right)+\frac{1}{U}\exp\left(\frac{E}{U}\right)$
	$T = 214\left(\frac{E_r}{3000}\right)0{\cdot}75$	
	$U = 0{\cdot}5(1+1{\cdot}07CE_r)\times 0{\cdot}285$ C = 1 for nuclear collisions C = 2 for pion collisions E_r = energy radiated in the collisions (GeV)	T and U calculated so that mean energies of forward and backward cones are equal in the CMS.

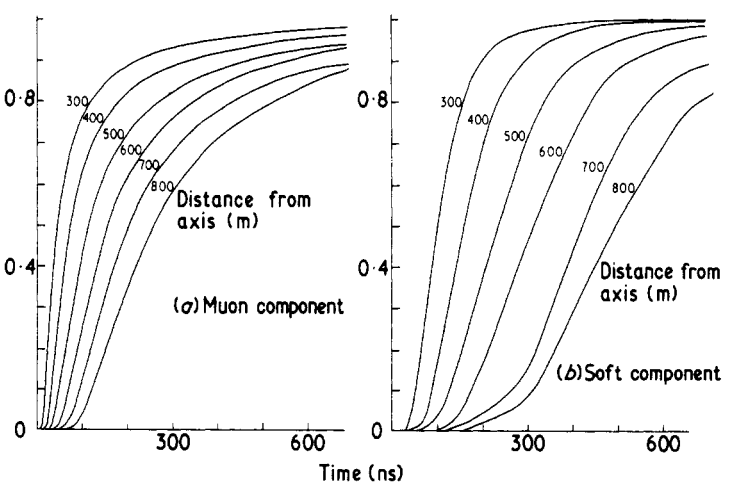

Figure 2. Integral time delay distribution of the detector signal for an average proton shower, $E_p = 1{\cdot}15 \times 10^{18}$ eV, $\theta = 0°$, calculated for model A. (*a*) Muon component of the detector signal; (*b*) soft component of the detector signal.

Table 3. Lateral distributions for an average proton shower: $\theta = 0°$, $E_p = 1{\cdot}15 \times 10^{18}$ eV, model A, as calculated by the author. ρ_μ is the muon component density; ρ_s is the soft component density; ρ is the total water-Čerenkov density; and ρ^* is the density when the finite decay time (approximately 5 μs) of the photomultiplier output signal is included in the calculation.

r_m	ρ_μ	ρ_s	ρ	ρ^*
50	85	2018	2103	2099
100	33	400	433	432
200	10·7	40	51	51
400	2·77	4·09	6·86	6·72
500	1·67	1·68	3·35	3·25
600	1·06	0·78	1·85	1·79
800	0·491	0·223	0·714	0·667
1000	0·267	0·071	0·338	0·320
1200	0·148	0·026	0·174	0·163
1600	0·052	0·002	0·054	0·049

3.1. Comparison with other calculations

3.1.1. Comparison with the results of Marsden. The reliability of the numerical calculations can be checked by comparing the present results with previous work by Marsden (1971), some of which has been previously published (Marsden *et al* 1971). Both sets of computations rely on the same three-dimensional electromagnetic cascade program; the other stages of the calculation were carried out using independent sets of computer programs. Particle density parameters are compared in table 4. The agreement between

Table 4. Comparison of particle densities calculated by Marsden (1971), DJM, and the author, JL. Model A, 10^{18} eV proton, $\theta = 0°$

Parameter	DJM	JL	Comments
Water-Čerenkov detector signal at $r = 500$ m	2·80 m^{-2}	2·91 m^{-2}	JL density obtained by dividing density for $E_p = 1{\cdot}15 \times 10^{18}$ eV by 1·15. Also Hillas *et al* (1971) give $\rho(500) = 2{\cdot}89$ m^{-2}.
Water-Čerenkov lateral distribution $\rho(r)/\rho(500)$			
$r = 100$ m	128	129	
$r = 1200$ m	0·052	0·053	
Muon/Čerenkov ratio at			$\mu/\check{C}$ not directly available from DJM for $E_p = 10^{18}$ eV. $\theta = 0°$; the values were obtained by interpolating between values at $\theta = 0°$, 25°, 35° with $E_p = 10^{17}$ eV; $\theta = 25°$ with $E_p = 10^{16}$, 10^{17}, 10^{18} eV.
$r = 250$ m	0·26	0·24	
$r = 400$ m	0·44	0·40	
$r = 600$ m	0·64	0·58	
$r = 1000$ m	0·81	0·76	

the two sets of results is good. The particle time delay distributions are compared in figure 3. There is here a gross inconsistency between the two sets of muon time profiles; this is attributable to Marsden having ignored velocity time delays in what was a preliminary investigation (Marsden *et al* 1971). The discrepancy between the soft component time delay distributions is small and can be attributed to the two distributions being for slightly different zenith angles and primary energies.

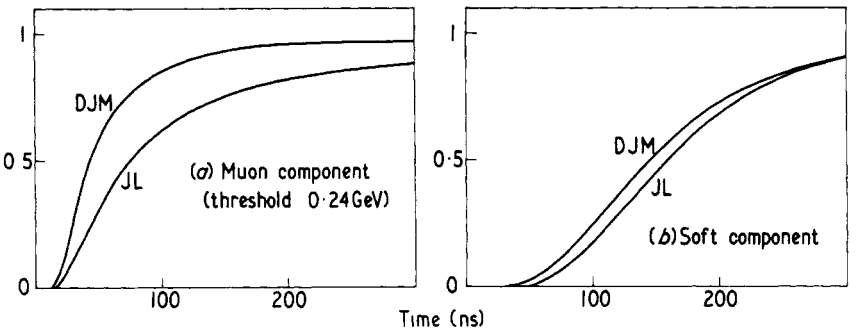

Figure 3. Comparison of the integral time distribution of (*a*) muons and (*b*) electrons at $r = 400$ m as calculated by the author (JL) and Marsden (DJM). Model A is used in both calculations; the DJM data are for an average proton shower of 10^{17} eV with $\theta = 25°$; the JL data are for an average proton shower of 10^{18} eV at $\theta = 0°$. The energy threshold for the muons is 0·24 GeV.

3.1.2 Comparison with the results of Dixon and Turver. Dixon and Turver (1974) (DT) have presented results on particle time delays in the form of median delay of muons relative to the tangent plane. Their results are compared with the present work in table 5, from which it is seen that the DT results are systematically faster than those calculated by the author. The two sets of values should, however, be expected to be different because:

(*a*) DT have not included velocity, scattering and geomagnetic delays; these effects form about 30% of the delay calculated in the present work.
(*b*) The DT calculations are for a muon detection threshold of 1 GeV compared with 0·24 GeV in the present work.
(*c*) The model used by DT is more like model E than model A (table 2).
(*d*) The DT calculation is for a primary energy of 10^{17} eV, while the present work is for 10^{18} eV for which the delays are about 10% larger.

Table 5. Comparison of t_{med} obtained by the author (JL) with that obtained by Dixon *et al* (DT); vertical shower (JL: 10^{18} eV; DT: 10^{17} eV).

Distance from axis (m)	t_{med} (JL) (ns)	t_{med} (DT) (ns)	t_{med} (JL)/t_{med} (DT)
300	45	33	1·4
400	74	50	1·5
500	115	79	1·5
600	162	123	1·3
1000	389	280	1·4

Thus the difference between the present results and those of Dixon and Turver is consistent with what can be expected from the differences in methods used and in the primary energy to which they refer.

3.2. Comparison with experiment

3.2.1. Muon/Čerenkov ratio, μ/Č. Measurements of the ratio of the muon density to the Čerenkov density in immediately adjacent tanks have been made at Haverah Park and were reported by Armitage *et al* (1973a). These measurements are compared with the present work in figure 4. The model results are shown for $\theta = 0°$, $\rho(500) = 0{\cdot}3\ \mathrm{m}^{-2}$ and $\rho(500) = 3\ \mathrm{m}^{-2}$. The experimental results are for $\theta = 25°$ and $\rho(500)$ of about $0{\cdot}3\ \mathrm{m}^{-2}$ at $r = 250$ m and $\rho(500)$ of about $2{\cdot}0\ \mathrm{m}^{-2}$ at $r = 800$ m. The experimental points are indicative of a slightly lower muon content than that predicted by the model. ($\rho(500)$ is the density of the Čerenkov signal at 500 m from the shower axis and is the parameter used to define shower size from the Haverah Park 500 m array (Edge *et al* 1973).)

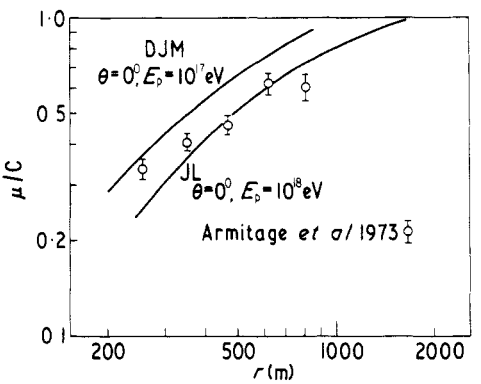

Figure 4. Comparison of the muon/Čerenkov ratio measured by Armitage *et al* (1973a) with the calculations of Marsden (DJM) and the author (JL). Model A used in both calculations: DJM, proton 10^{17} eV, $\theta = 0°$: JL, proton 10^{18} eV, $\theta = 0°$.

3.2.2. Water-Čerenkov lateral distribution. Figure 5 compares the lateral distribution of the deep water-Čerenkov signal measured at Haverah Park (Edge *et al* 1973) with that predicted by model A for $E_p = 10^{17}$, 10^{18}, 10^{19} eV. The measurements for $r \simeq 100$ m were derived from showers with $\rho(500) \simeq 0{\cdot}4\ \mathrm{m}^{-2}$ ($E_p \simeq 10^{17}$ eV) and the measurements for the large distances, $r \simeq 1200$ m, for showers with $\rho(500) \simeq 10\ \mathrm{m}^{-2}$. The measurements are seen to agree well with the model.

3.2.3. Water-Čerenkov time profile. Measurements of the time profile of the deep water-Čerenkov detector signal have been made at Haverah Park, results having been reported by Lapikens *et al* (1973) and Watson and Wilson (1974). When comparing these measurements with model calculations it is important to emphasise that the response time of the detectors is not fast compared with the particle delays being studied and that the detector and electronic recording system characteristics can therefore make a significant contribution to the observed pulse shapes. If the response function $S(t)$ of the recording

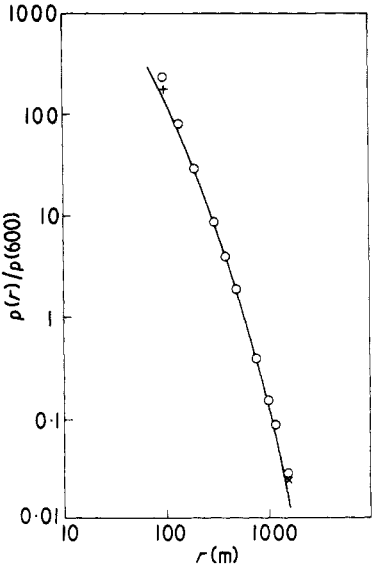

Figure 5. Comparison of the measured water-Čerenkov detector lateral distribution (Edge *et al* 1973) with the present calculations for protons for 10^{17} eV, + ; 10^{18} eV, ○ ; and 10^{19} eV, × ; all at $\theta = 0°$. The experimental data are for $\theta < 20°$ and for a range of energies as discussed in the text.

system to a δ-function input is known, then the effect of the system on a particle time profile $D(t)$ can readily be calculated as follows:

$$V(t) = \int_0^t S(t-t')D(t')\,dt'.$$

The response function of the Haverah Park recording system has been determined by observing the pulses produced by the traversal of single muons through the detector. The observed $S(t)$ and its effect on the time profile at $r = 500$ m from an average proton shower are illustrated in figure 6.

The variation of the rise-time parameter $t_{1/2}$ (the time for the signal to rise from 10% to 50% of its full height) with distance from the shower axis is shown superimposed on a sample of measurements of $t_{1/2}$ for individual air shower pulses made by Watson and Wilson (1974) in figure 7. The measurements are consistent with the predictions of the model.

3.2.4. Muon time profile. Armitage *et al* (1973b) have made measurements of the arrival times of individual muons traversing 1·2 m^2 scintillators relative to the arrival time of the 'first detectable signal' in an adjacent Haverah Park 34 m^2 deep water-Čerenkov detector. From several hundred such measurements they formed muon arrival-time distributions for various zenith angle and distance ranges. These results cannot be considered to be direct measurements of the muon time delay distribution because the times were measured relative to the 'start' of the adjacent deep water-Čerenkov detector signal—a point in time which varies with Čerenkov-density and distance from shower axis and is uncertain because only a small sample of particles has produced the Čerenkov pulse shape. These variations, combined with instrumental uncertainties of 20 ns, will tend to produce a broadened distribution of observed muon times. To compare

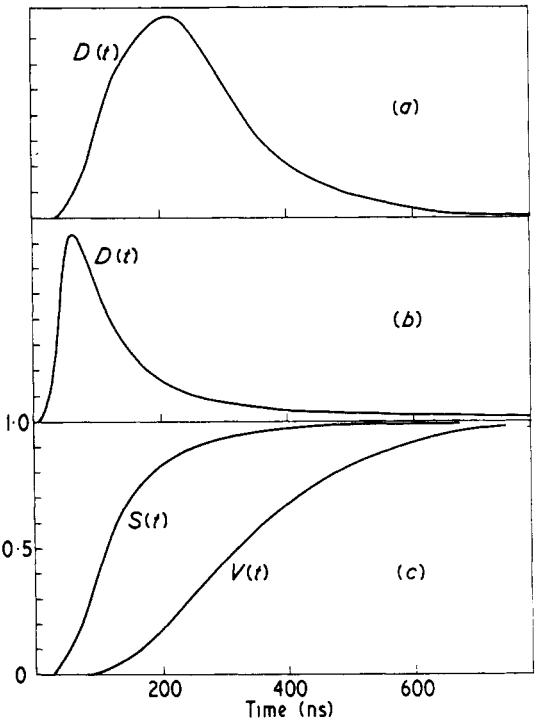

Figure 6. Water-Čerenkov time profile for average proton, $E_p = 10^{18}$ eV, $\theta = 0°$ at 500 m from the shower axis.

(*a*) Differential time distribution of the deep water-Čerenkov detector signal produced by the electron–photon component.

(*b*) Differential time distribution of the deep water-Čerenkov detector signal produced by muons.

(*c*) $S(t)$ is the response of the recording system to an instantaneous input signal. $V(t)$ is the pulse which would be observed by the recording system from a signal containing 50% of muons and 50% of the electron–photon component.

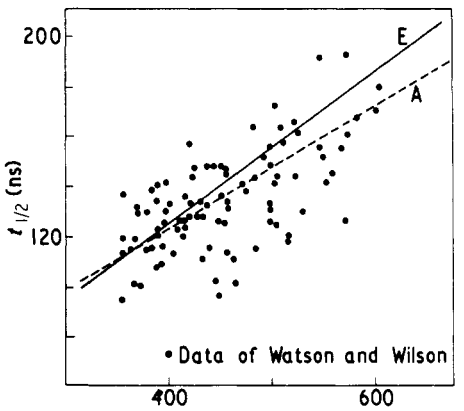

Figure 7. Comparison of the average value of $t_{1/2}$ as a function of distance for models A and E with the experimental data of Watson and Wilson (1974) for showers with $\theta < 20°$. The calculations are for proton showers of 10^{18} eV in the vertical direction. There has been no normalization of theory to experiment.

the results of the calculations with the experiment of Armitage *et al*, we must make an estimate of the broadening effect caused by using an ill-defined time origin (the 'start' of the Čerenkov pulse). Such an estimate can be derived from the muon and soft component time delay distributions predicted by the model calculations. The method is described in detail by Lapikens (1974); for measurements on near-vertical showers in the distance interval 400 to 500 m it is estimated that the 'start' of the Čerenkov pulse is uncertain to about 25 ns. This result has been used to produce a modified muon time distribution from the model calculation results which is directly comparable with the observations of Armitage *et al.*

The theoretical muon time distribution at $r = 450$ m, with the previously described broadening effects included, is shown in figure 8; also shown is the time distribution measured by Armitage *et al* for the range $400 < r < 500$ m, $\theta < 25°$. The two curves agree well, bearing in mind the difficulties of an exact comparison.

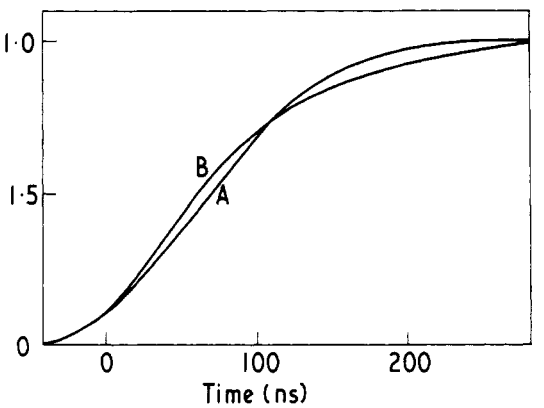

Figure 8. Comparison of the muon time delay measurements of Armitage *et al* (1973b) with the results of model calculations. Curve A: Armitage *et al*, $\theta < 25°$, $400 < r < 500$ m. Curve B: this paper, $\theta = 0°$, $r = 450$ m, model A with measurement errors added.

Armitage *et al* (1973b) claimed that their results agreed with the work of Marsden (1971) which was shown above (§ 3.1.1.) to be in contradiction with the present work. The comparison of Armitage *et al* was however only made at the 10% and 90% points of the rise time and was not as detailed as that attempted here.

4. Calculation of the fluctuations present in proton-induced EAS

Watson and Wilson (1974) have demonstrated that fluctuations of $t_{1/2}$ at distances of approximately 450 m from the axis exist between showers which are significantly greater than those expected on the basis of measurement errors and statistical sampling effects alone. They make an estimate of the fluctations which are due to shower development factors and it is the purpose of this section to describe how this estimate compares with that predicted for fluctuations in the development of proton-initiated EAS.

A good starting point for approaching such a problem (Marsden *et al* 1971) is to examine the features of a group of simulated proton-induced showers, with the mean free path and inelasticity often assumed for low energy protons ($\lambda = 80\,\mathrm{g\,cm^{-2}}$,

$k = 0{\cdot}19 + 0{\cdot}5R$, where R is a random number between 0 and 1). To economize on computing time, proton-induced showers with randomly selected interaction points and inelasticities of the primary particle did not have their particle densities calculated directly but were built up by interpolating between the results of calculations for a proton shower which interacted once only at various depths, 25, 50, 100, 150..., 650, 700 g cm^{-2} in the atmosphere. Such a method makes the approximation that the particle density at ground level, resulting from a collision of the primary proton, is proportional to the energy radiated in the collison and does not therefore give exact results. Tests which compare the results of approximate calculations with 'exact' results have, however, shown that the approximate method predicts the magnitude of fluctuations of observables to an accuracy of better than 10% (Lapikens 1974). All fluctuation phenomena considered here are therefore derived from the characteristics of a small number of 'unnatural' showers for which the primary proton interacted once only at a specified depth g_s in the atmosphere. The characteristics of these showers were calculated by the techniques outlined in § 2.

A sample of results shown in figure 9 illustrates how the normalized muon and soft component profiles become slower with increasing g_s. It can be seen that the muon time delays are more sensitive to variation of g_s than are soft component time delays. Figure 10 shows how particle densities vary with g_s; the fluctuations in lateral distribution can also be derived from this diagram.

Several hundred proton-induced showers were simulated and the pulse profile that would be observed at various axial distances was calculated for each shower. The standard deviation $\sigma_f(r)$ of the time parameter $t_{1/2}$ for these simulated profiles is shown in figure 11. Watson and Wilson found values corresponding to σ_f of $5{\cdot}8 \pm 1{\cdot}3$ ns for showers of primary energy of the order 5×10^{17} eV, mean zenith angle 25° and mean distance 435 m, and $9{\cdot}9 \pm 1{\cdot}8$ ns for showers of primary energy of the order $1{\cdot}5 \times 10^{18}$ eV, mean zenith angle 25° and mean distance 465 m. The measured fluctuations thus agree closely with those predicted for a pure proton composition on the basis of the shower model used here, ie about 7 ns at 500 m.

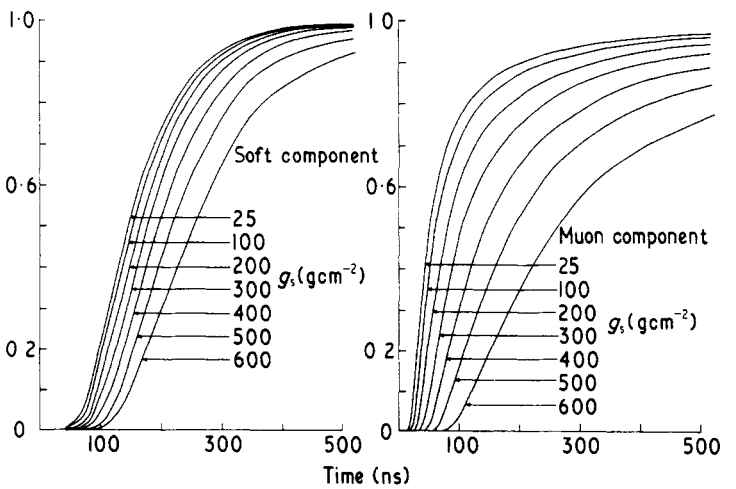

Figure 9. Time delay distributions of the soft and muon components for a proton which interacts once only at g_s g cm^{-2}, r = 400 m, $\theta = 0°$, $E_p = 1{\cdot}15 \times 10^{18}$ eV (model A).

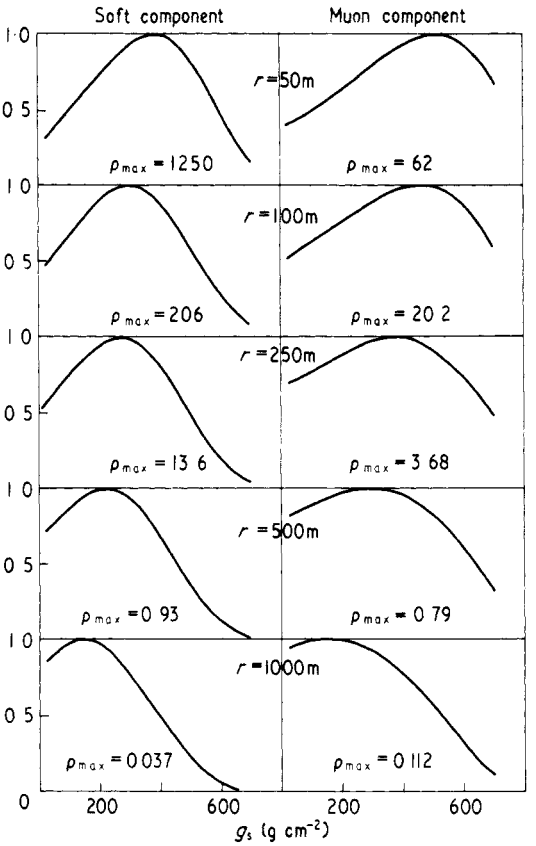

Figure 10. Variation of the soft component and muon component as a function of g_s, the depth of the only interaction, for a vertically incident proton of $1{\cdot}15 \times 10^{18}$ eV (model A). Ordinates normalized to maximum.

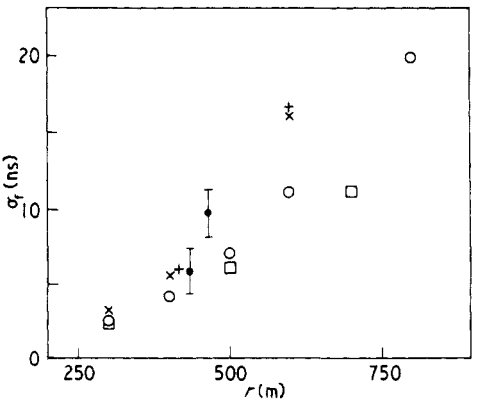

Figure 11. Comparison of the fluctuation σ_f of the parameter $t_{1/2}$ for models A and E and various showers produced by protons.

○ $\theta = 0°$ $E_p = 10^{18}$ eV
× $\theta = 25°$ $E_p = 10^{17}$ eV } model A { based on present work.
\+ $\theta = 25°$ $E_p = 10^{17}$ eV } { based on Hillas *et al* (1971).
□ $\theta = 0°$ $E_p = 10^{18}$ eV model E
Experimental data, Watson and Wilson (1974).

Fluctuations in showers initiated by nuclei heavier than protons are expected to be smaller than proton-initiated EAS. An indication of the decrease in the fluctuations as a function of A, the atomic mass, can be gained from consideration of the detailed work of Dixon and Turver (1974) on this problem. They find that the fluctuations of various quantities (the number of muons, the number of electrons and the depth of shower maximum) in a shower produced by α particles are about half the corresponding fluctuations for proton showers. (For nuclei *heavier* than α particles Dixon and Turver show that fluctuations decrease only rather slowly with increasing mass.) Hence *if* the fluctuations in $t_{1/2}$ are also reduced by two in α particle EAS over that found in proton EAS *then* the data of Watson and Wilson support the view that protons dominate in the primary beam at these energies.

5. Calculations with other models

The results described above all derive from a calculation using one particular model, model A, the details of which are described in table 2, and the choice of this model was partly dictated by the opportunity to have the detailed check of computational accuracy provided by comparison with the work of Marsden (1971). There is growing evidence, however, that calculations based on model E provide a better description of the shower phenomena above 10^{17} eV. For example the muon content in EAS is more accurately predicted with model E than with model A (Hillas *et al* 1971). The two models differ mainly in that in model A twice as many low energy as high energy pions are radiated (see table 2).

The techniques described above have been repeated using model E to calculate the mean variation of $t_{1/2}$ with distance and width of the time fluctuations in proton-initiated EAS. As seen in figure 7 the mean variations predicted by the two calculations are indistinguishable with the present experimental data. The values of $\sigma_f(r)$ are slightly different (figure 11) for the two models but at present the experimental work is not sufficiently accurate to distinguish between them. It is important to note that the change in σ_f between two (rather similar) models is much less than the change expected in σ_f for a change in primary mass.

The manner in which σ_f varies between models is clearly a most important subject for future detailed calculations. A study of this problem has been made in a general way since the range of possible models is exceedingly large. Model variations were represented by two parameters:

(i) A change in the depth of atmosphere, roughly equivalent to a change in zenith angle, was used to investigate the effect of increasing the rate of shower growth which might occur if the multiplicity was increased or decreased.

(ii) A change in the proportion of muons, $\mu/\check{C}$, which contribute to the total water-Čerenkov signal.

At $r = 400$ m the observed value of $\mu/\check{C}$ is 0·4 (Armitage *et al* 1973a). Performing a fluctuation calculation for σ_R, the $t_{1/2}$ fluctuation parameter, with $\mu/\check{C} = 0{\cdot}6$ and 0·25 showed that σ was increased and decreased by 40% respectively. A similar calculation for a shift of $\pm 150\ \mathrm{g\,cm^{-2}}$ in the atmospheric depth caused a change of 20% in the $t_{1/2}$ fluctuations, mainly through its effect of changing the muon/Čerenkov ratio. It may be concluded, therefore, that the predicted rise-time fluctuations are accurate to within 30% independent of a knowledge of the shower model.

More detailed studies using specific models are clearly needed. An early effort should be made to carry through calculations using the scaling model, and a detailed study of the effect of changing the proton mean free path is also particularly important.

6. Conclusions

In this paper a rapid method of calculating the fluctuations in the time profile of EAS has been developed with particular reference to the deep water-Čerenkov detectors at Haverah Park for which studies of this profile are possible. Care has been taken to allow the model calculation to be matched with the experimental data of Watson and Wilson (1974), and the conclusion of those authors that protons are present in the cosmic ray beam at about 10^{18} eV is supported. Indeed on the basis of two rather similar models the experimental data would be consistent with a predominantly protonic beam, but further model studies, in parallel with the more advanced experimental developments referred to by these authors, are required before this conclusion can be regarded as fully established.

Acknowledgments

I should like to thank the Science Research Council for a studentship and for the oportunity of using the facilities at Haverah Park. The present work has benefitted from discussions with many Leeds colleagues in the Haverah Park collaboration.

References

Armitage M L, Blake P R and Nash W F 1973a *J. Phys.* A: *Math., Nucl. Gen.* **6** 878–85

—— 1973b *Proc. 13th Int. Conf. on Cosmic Rays, Denver* vol 4 (Denver: University of Denver) pp 2545–50

Baxter A J 1969 *J. Phys.* A: *Gen. Phys.* **2** 50–8

Dixon H E and Turver K E 1974 *Proc. R. Soc.* A **339** 171–95

Edge D M, Evans A C, Garmston H J, Reid R J O, Watson A A, Wilson J G and Wray A M 1973 *J. Phys.* A: *Math., Nucl. Gen.* **6** 1612–34

Hillas A M 1965 *Proc. 9th Int. Conf. on Cosmic Rays, London* vol 2 (London: The Institute of Physics and the Physical Society) pp 758–61

Hillas A M, Hollows J D, Marsden D J and Hunter H W 1971 *Proc. 12th Int. Conf. on Cosmic Rays, Hobart* vol 3 (Hobart: University of Tasmania) pp 1007–12

Lapikens J 1974 *PhD Thesis* University of Leeds

Lapikens J, Watson A A, Wild P and Wilson J G 1973 *Proc. 13th Int. Conf. on Cosmic Rays, Denver* vol 4 (Denver: University of Denver) pp 2582–7

Linsley J and Scarsi L 1962 *Phys. Rev.* **128** 2384–92

Marsden D J 1971 *PhD Thesis* University of Leeds

Marsden D J, Hillas A M, Hollows J D and Hunter H W 1971 *Proc. 12th Int. Conf. on Cosmic Rays, Hobart* vol 3 (Hobart: University of Tasmania) pp 1013–8

Watson A A and Wilson J G 1974 *J. Phys.* A: *Math., Nucl. Gen.* **7** 1199–212

Wilson J G, Allan H R, Lillicrap S C, Reid R J O and Turver K E 1963 *Proc. 8th Int. Conf. on Cosmic Rays, Jaipur* vol 4 (Bombay: TIFR) pp 27–34